Tellus (2003), 55B, 197–206
Printed in UK. All rights reserved

TELLUS
ISSN 0280–6509

The atmospheric signal of terrestrial carbon isotopic discrimination and its implication for partitioning carbon fluxes

By JOHN B. MILLER[1,2]*, PIETER P. TANS[1], JAMES W. C. WHITE[2], THOMAS J. CONWAY[1] and BRUCE W. VAUGHN[2], [1]*Climate Monitoring and Diagnostics Laboratory, National Oceanic and Atmospheric Administration, Boulder, Colorado, USA;* [2]*Institute for Arctic and Alpine Research, University of Colorado, Boulder, Colorado, USA*

(Manuscript received 17 January 2002; in final form 2 September 2002)

ABSTRACT

The ^{13}C:^{12}C ratio in atmospheric carbon dioxide has been measured in samples taken in the NOAA/CMDL network since 1991. By examining the relationship between weekly anomalies in $\delta^{13}C$ and CO_2 at continental sites in the network, we infer temporal and spatial values for the isotopic signature of terrestrial CO_2 fluxes. We can convert these isotopic signatures to values of discrimination if we assume the atmospheric starting point for photosynthesis. The average discrimination in the Northern Hemisphere between 30 and 50°N is calculated to be 16.6 ± 0.2 per mil. In contrast to some earlier modeling studies, we find no strong latitudinal gradient in discrimination. However, we do observe that discrimination in Eurasia is larger than in North America, which is consistent with two modeling studies. We also observe a possible trend in the North American average of discrimination toward less discrimination. There is no apparent trend in the Eurasian average or at any individual sites. However, there is interannual variability on the order of 2 per mil at several sites and regions. Finally, we calculate the northern temperate terrestrial CO_2 flux replacing our previous discrimination values of about 18 per mil with the average value of 16.6 calculated in this study. We find this enhances the terrestrial sink by about 0.4 GtC yr^{-1}.

1. Introduction

Measurements of atmospheric CO_2 mole fraction tell us that only about half the CO_2 derived from fossil-fuel combustion remains in the atmosphere; the other half is absorbed at the surface of the earth (Marland et al., 1993). Combining measurements of $\delta^{13}CO_2$ with CO_2 allows us to estimate the terrestrial and oceanic components of the surface sink. This partitioning is possible because uptake of CO_2 by terrestrial (C_3) plants discriminate against ^{13}C by about 18‰, whereas uptake by the oceans discriminates by about only 2‰.

For partitioning, we also need to estimate accurately the contribution of oceanic and terrestrial isotopic fluxes associated not with net carbon exchange but with gross exchanges between reservoirs (Tans et al., 1993). These "disequilibrium" fluxes arise from time lags in the isotopic composition of the oceanic and terrestrial reservoirs relative to the atmosphere and are the result of increasing fossil fuel emissions and land-use changes.

Once we have estimates for the discrimination and disequilibrium terms, we can use global CO_2 and $\delta^{13}C$ measurements to deduce global oceanic and terrestrial CO_2 uptake. Using an inverse model of atmospheric transport these fluxes can be decomposed into spatial patterns. For the purposes of this study, it is important to note that the $\delta^{13}C$ and CO_2 inputs to the

*Corresponding author.
e-mail: john.b.miller@noaa.gov

model are smoothed over time and do not include the high-frequency variability that exists in the data. Here, we will take advantage of these high-frequency components and estimate terrestrial isotopic discrimination by correlating high-frequency variations in CO_2 and ^{13}C. This method avoids potential circularities in applying the measurements to the partitioning method.

Our first goal in this study is to use atmospheric observations to check patterns of terrestrial isotopic discrimination that have been derived using ecophysiological models. This work updates and extends the analysis of Bakwin et al. (1998). Lloyd and Farquhar (1994), Fung et al. (1997) and Suits et al. (personal communication, 2002) have constructed global models of terrestrial isotopic discrimination. These models are all based on the model of photosynthetic fractionation developed by Farquhar et al. (1989). Inputs to the Lloyd and Farquhar model include temperature, humidity and precipitation as well as gross primary production. In the approach of Fung et al. (1997), these fields are calculated using a general circulation model coupled to a biospheric model; the model of Suits et al. (personal communication 2002) is a more sophisticated version of the Fung et al. (1997) approach. Both general approaches require the specification of the amount of assimilation by C_4 plants in each model grid cell. Calculation of terrestrial discrimination is sensitive to the prescribed proportion of C_3/C_4 photosynthesis, because C_3 plants discriminate by about 18‰ whereas C_4 plants discriminate by about only 4‰. In contrast, our method specifies nothing about the terrestrial biosphere; we focus only on the imprint of discrimination on the atmosphere. Our second goal is to compare the terrestrial and oceanic fluxes determined using various modeled values of discrimination and our values calculated from observations.

2. Methods

2.1. Sample collection and analysis

All the data used in this study were obtained from air samples collected as part of the NOAA/CMDL Cooperative Air Sampling Network. The subset of sites studied is listed in Table 1. The sample collection procedures have been described in detail previously (e.g. Conway et al., 1994). Typically, air is pumped into a pair of 2.5 L glass flasks, connected in series, and filled to slightly above local ambient pressure. All data analyzed here are the average of such pairs. The only pair data not used here are those that have been flagged because of known sampling or analysis problems. In addition, when the difference between members of a pair exceeds a pre-determined threshold (0.5 ppm for CO_2 and 0.15‰ for $\delta^{13}C$), the data are also excluded from further analysis. The analysis of CO_2, $\delta^{13}C$ and CO has also been described in detail previously, by Conway et al. (1994), Trolier et al. (1996) and Novelli et al. (1998). The respective analytical precision for each of these species is 0.1 ppm, 0.01‰ and 1 ppb.

Table 1. *NOAA/CMDL continental sampling stations*

No.	Code	Location	δ_{bio}(‰)	Lat. (°N)	Lon. (°E)	Altitude (m asl)
1	ASK	Assekrem, Algeria	−27.67	23.18	5.42	2728
2	BAL	Baltic Sea, Poland	−25.96	55.50	16.67	7
3	BSC	Black Sea, Romania	−23.02	44.17	28.68	3
4	HUN[1]	Hegyhatsal, Hungary	−23.50	46.95	16.65	344
5	ITN[1]	North Carolina, USA	−24.49	35.37	−77.39	505
6	KZD	Plateau Assy, Kazakstan	−24.91	44.45	77.57	412
7	KZM	Sary Taukam, Kazakstan	−25.14	43.25	77.88	2519
8	LEF[1]	Wisconsin, USA	−24.43	45.93	−90.27	868
9	NWR	Colorado, USA	−23.23	40.05	−105.58	3475
10	TAP	Tae-anh Peninsula, Korea	−25.16	36.73	126.13	20
11	UTA	Utah, USA	−20.23	39.90	−113.72	1320
12	UUM	Ulaan Uul, Mongolia	−23.74	44.45	111.10	914
13	WIS	Negev Desert, Israel	−24.46	31.13	34.88	400
14	WLG	Mt. Waliguan, China	−26.15	36.29	100.90	3810

[1]Tall tower sampling sites.

2.2. *Data analysis model*

We relate changes in CO_2 and $\delta^{13}C$ to infer isotopic discrimination in a source or sink. This strategy is similar to the two end-member mixing model of Keeling (Keeling, 1961) with the important difference that our approach allows for a time-varying background of CO_2 and $\delta^{13}C$. The "Keeling plot" approach assumes a constant background concentration and $\delta^{13}C$ of CO_2, which is violated when analyzing a time-series. The calculation approach used here is described in detail in an accompanying paper (Miller and Tans, 2002). We also test a method that corrects for the recent fossil fuel contribution to the samples similar to that employed by Bakwin et al. (1998).

We define the observed CO_2 mole fraction to be the sum of contributions from some regional background and regional fluctuations due to biospheric sources and sinks and fossil fuel emissions. We define a similar equation for the product of CO_2 and $\delta^{13}C$ (Tans, 1980). Like ^{13}C, the product of $\delta^{13}C$ and CO_2 is conservative, whereas $\delta^{13}C$ is not.

$$C_{\text{obs}} = C_{\text{bg}} + C_{\text{ff}} + C_{\text{bio}} \tag{1}$$

$$\delta_{\text{obs}} C_{\text{obs}} = \delta_{\text{bg}} C_{\text{bg}} + \delta_{\text{ff}} C_{\text{ff}} + \delta_{\text{bio}} C_{\text{bio}}. \tag{2}$$

For each sampling site, a curve consisting of a second-order polynomial and two harmonic functions is fitted to the data (Thoning et al., 1989). The residuals from the fit are then smoothed in frequency space using a short-term cutoff filter of 80 d and a long-term filter of 334 d (both filters full-width at half-maximum, FWHM). The smoothed residuals are then added back to the curve. We interpret the "smooth curve" as representing a regional average for either CO_2 or $\delta^{13}C \times CO_2$, so the background components in eqs. (1) and (2), C_{bg} and $\delta_{\text{bg}} C_{\text{bg}}$, are defined by the smooth-curve fits to the data. We also interpret the residual differences between the observations and the smooth-curve fit to be representative of processes occurring on a regional scale.

In eqs. (1) and (2) we do not make explicit any contribution to the observed signals resulting from air–sea gas exchange. We justify this by focusing on observing stations located on the continents, and restricting our analysis to the differences between the data and the smooth-curve fit. We observe an oceanic signal, but we assume that this signal contributes only to the background concentration and isotope ratio and therefore does not contribute to the difference between the data and smooth curve.

If we make the additional simplification of ignoring the fossil fuel terms in eqs. (1) and (2), we can derive an equation for δ_{bio} by rearranging eq. (2):

$$\delta_{\text{obs}} C_{\text{obs}} - \delta_{\text{bg}} C_{\text{bg}} = \delta_{\text{bio}} (C_{\text{obs}} - C_{\text{bg}}). \tag{3}$$

However, we can estimate C_{ff} and calculate C_{bio} by taking advantage of CO measurements made on the same air used to determine CO_2 and $\delta^{13}C$. If we know the molar emission ratio of CO to CO_2, R, for fossil fuel combustion, we can estimate C_{ff} according to eqs. (4) and (5).

$$CO_{\text{obs}} = CO_{\text{bg}} + CO_{\text{ff}} \tag{4}$$

$$C_{\text{ff}} = \frac{CO_{\text{obs}} - CO_{\text{bg}}}{R}. \tag{5}$$

As with CO_2, CO_{bg} is defined to be the smooth curve fit to the CO data. Figure 1 shows the sample data (before and after the fossil fuel correction has been applied) and smooth-curve fits for CO_2, $CO_2 \times \delta^{13}C$ and CO for the LEF site. Also shown are the residuals of the CO_2 and $CO_2 \times \delta^{13}C$ fits. We neglect changes in CO due to OH photochemistry, biomass burning and hydrocarbon oxidation. Bakwin et al. (1998) showed that changes in CO:CO_2 emission ratios of 15% and the inclusion of OH consumption had very little effect on the calculation of δ_{bio}. Here we take a value for R of 20 ppb CO/ppm CO_2, which is consistent with both inventory estimates and atmospheric data (Bakwin et al., 1998; Potosnak et al., 1999).

We now combine eqs. (1), (2) and (5) to give eq. (6):

$$(\delta C)^{\text{r}} - \frac{\delta_{\text{ff}} CO^{\text{r}}}{R} = \delta_{\text{bio}} \left(C^{\text{r}} - \frac{CO^{\text{r}}}{R} \right). \tag{6}$$

Values for δ_{ff} are taken from a zonally and annually averaged data set of $\delta^{13}C$ of fossil-fuel emissions for 1992 (Andres et al., 1996). For a given site, values from the four nearest 1° zonal bands are averaged to calculate δ_{ff}. Superscript r denotes the residual difference between the data and smooth curve. The value of δ_{bio} is not highly sensitive to the value of δ_{ff}. Changing δ_{ff} by 2.0‰ yields a change in δ_{bio} of only 0.4‰, on average. The right-hand-side of eq. 6 is plotted against the left such that the slope of the line is δ_{bio}. Figure 2 shows the residual data from Fig. 1 plotted using eqs. (3) and (6).

To test the effect of our fossil-fuel correction we first calculate the change in the standard deviation of the residuals due to the fossil-fuel correction for both summer and the winter. In the winter months (December–March) the fossil-fuel correction significantly reduces

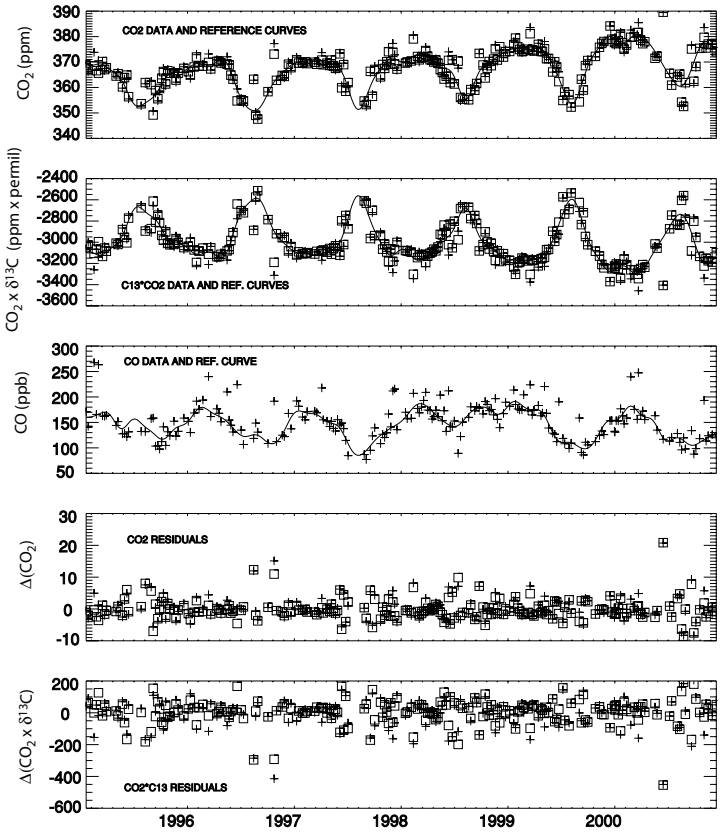

Fig. 1. CO_2, $\delta^{13}C \times CO_2$, and CO data from sampling station LEF between 1995 and 2001. In the top two panels pluses represent averages of pairs of flask samples, and squares represent those averages with a fossil-fuel correction applied. The solid lines in the top three panels are the "smooth-curve" fits to the uncorrected data. In the bottom two panels, the pluses represent the differences between the uncorrected data and the smooth curve, and the squares represent the differences between the corrected data and the smooth curve.

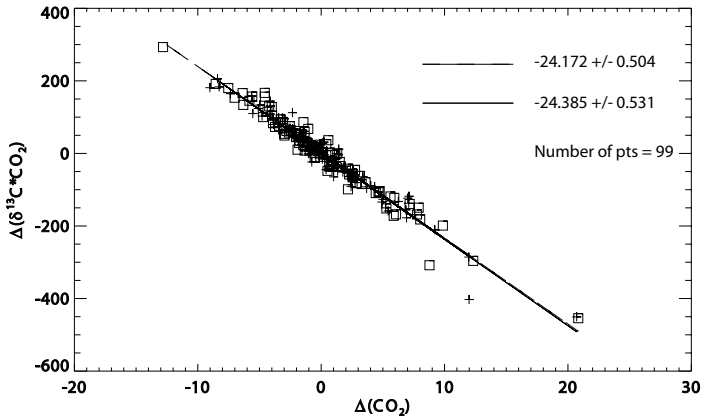

Fig. 2. Regressions of the data in the bottom two panels in Fig. 1 with reduced major axis regressions fit through each set of corrected (squares and dashed line) and uncorrected data (pluses and solid line).

the standard deviation of the data about the smooth curve, while in the summer (May–September) there is either no change or even an increase. This result is consistent with the idea that most of the variance during the winter is due to fossil-fuel emissions, while the summertime variance is due mainly to biological emissions. We also compare the values of δ_{bio} with and without the fossil-fuel correction. During the winter, no sites exhibit statistically significant differences ($P < 0.05$) in δ_{bio} calculated with and without the fossil-fuel correction. During the summer, the values of δ_{bio} with and without the fossil-fuel correction are also remarkably similar. Only at UUM is there a significant difference ($P < 0.05$). The 3‰ difference is due to high values of CO that are not correlated with high values of CO_2. This is likely a result of biomass burning. The 20 ppb CO/ppm CO_2 value of R is most likely too small for biomass burning, and as a result we greatly overestimate C_{ff}. An examination of data from other sites also reveals the same biomass burning problem. Our preferred approach, therefore, is to use eq. (3) to solve for δ_{bio}, and to analyze data only from the summer months, when the variance in the CO_2 and $\delta^{13}C$ signals are probably dominated by biological activity. Examining data only during the summer, when terrestrial fluxes are largest relative to oceanic ones, also minimizes the contribution of air–sea gas exchange.

2.2.1. Curve fitting. The line is fit using a regression which takes into account uncertainty in both x and y (sometimes referred to as "Model II"). This technique returns the inverse of the slope when the axes are reversed, giving us confidence that the fit is accurate, which is not the case with an ordinary least-squares regression. Lines fit using a least-squares method, or any method that assumes there is no error in x, result in slopes that are not steep enough, and thus values for δ_{bio} that are systematically too positive.

In addition to the slope itself, it is important to accurately estimate the slope uncertainty. If one prescribes uncertainties derived from the analytical precisions of CO_2 and $\delta^{13}C$ a subsequent chi-square test for goodness of fit typically yields chi-square probability values less than 0.1. This is a strong indication that the uncertainty estimates for the data are too small, which is consistent with the observed variability being dominated by "natural" variability and not measurement error. To obtain reasonable error estimates for δ_{bio}, we scale the x and y errors until the chi-square test returns a chi-square probability of about 0.5. These new error bars more accurately reflect the combination of uncertainty associated with measurement and the appropriateness of the model we use [eq. (5)] to the data. This process is described in detail in a companion paper (Miller and Tans, 2002). We believe that our method yields reasonable values for δ_{bio} and its uncertainty.

2.3. Footprint of δ_{bio}

That we are looking only at deviations from the smooth-curve fit to the data probably restricts our analysis to processes occurring relatively close to the observing station. In contrast, examining differences between the data and the long-term trend (also derived by smoothing residuals with the filters described above) would enlarge the temporal and spatial scale of the analysis. Nonetheless, the question remains: What is the footprint of these anomalies relative to the smooth curve? A footprint analysis of the LEF sampling station. (Gloor et al., 2001) has shown the station to be primarily influenced by a region of order 10^6 km^2, i.e. a radius of about 500 km. Since this analysis used C_2Cl_2 as a tracer, which does not have any local surface sources, the footprint with respect to CO_2 is likely to be smaller. This 10^6 km^2 scale is likely applicable to other continental stations with similarly high residual standard deviations of 4–6 ppm (BAL, BSC, HUN, ITN and TAP). The remaining high-altitude and desert stations with significantly lower residual standard deviations (2–3 ppm) likely have a larger footprint.

The most important way in which our analysis restricts the spatial scale of δ_{bio} calculated at each site is that the larger anomalies relative to the smooth curve are most likely to originate closer to the sampling location. Conversely, the farther away a source or sink of CO_2 is, the more likely its atmospheric signal is to be damped by atmospheric mixing prior to reaching the sampling location. In curve fitting, the points at the ends are the most important in determining the slope of the curve. In our case, these end points correspond to the larger, and thus more proximal, CO_2 and $\delta^{13}C$ anomalies used to calculate δ_{bio}.

3. Results and discussion

3.1. Meridional variations

Figure 3 shows δ_{bio} for the subset of continental sites during May–September for which more than three years of data were available. δ_{bio} varies from about −28 to−20‰, with most sites having values in the range of −26 to −23‰. The mean of the 14 sites

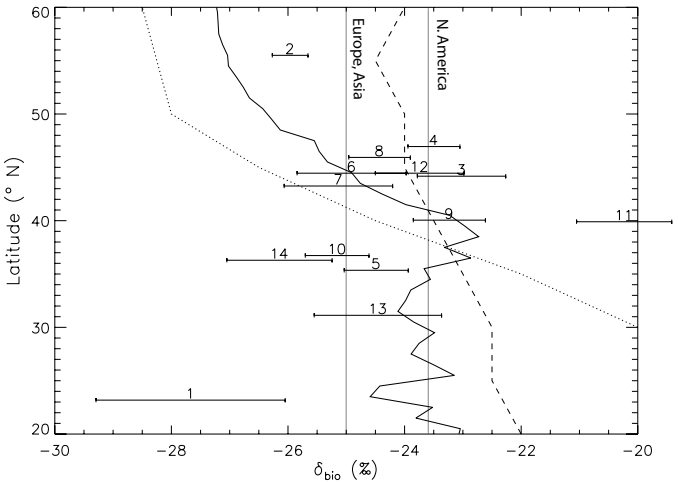

Fig. 3. Calculated values of the terrestrial isotopic signature as a function of latitude. Each number refers to a site in Table 1. These are the slopes from the regression of uncorrected data shown in Fig. 2 applied to all continental sites with more than 3 yr of data. Error bars are standard errors of each regression slope scaled to account for "natural variability" (see text). Also shown are the average slopes when all the sites in each of Europe, Asia and North America are binned together. Europe and Asia have the same slope. The lines are zonal mean values of discrimination calculated by the following models: Fung et al. (1997) dotted; Suits et al. (personal communication, 2002) solid; Lloyd and Farquhar (1994) dashed.

is -24.9 ± 1.9‰ (one sigma standard deviation between sites). The mean of all the sites, when the data are weighted according to the square of the uncertainty, is -24.6 ± 0.2‰ (here, the uncertainty is estimated by propagating individual site uncertainties through the weighted mean calculation). The latter average is slightly heavier than the first, because sites with large uncertainties for δ_{bio}, like ASK, and WLG have the most negative values for δ_{bio}. Assuming an atmospheric starting point for discrimination of about -8‰, and no terrestrial isotopic disequilibrium, these values of δ_{bio} correspond to isotopic discrimination values of slightly less than 17‰.

Two sites stand out in Fig. 3, UTA and ASK. Samples from UTA could be influenced by ecosystems with a large fraction of C_4 photosynthesis. Additionally, the aridity of the western US might result in values of C_3 discrimination that are significantly smaller than the global average. However, NWR, also in the western US, has a more negative average δ_{bio} than UTA. The ASK sampling site, located in the Sahara Desert, is much different than all other continental sites because it is so far removed from large terrestrial sources and sinks of CO_2. The variance of CO_2 about the smooth curve at ASK is similar to that of an oceanic sampling site. Here our assumption that terrestrial biology is the dominant contributor to variance about the smooth curve may not hold.

So far, we have combined high- and low-altitude sites. To test whether there is difference between the high- and low-altitude sites (using 2000 m as the dividing line), we calculate the respective weighted means. The four high-altitude sites, ASK, KZM, NWR and WLG, have an average value of δ_{bio} of -24.6 ± 0.4, while the remaining low-altitude sites have an average value of δ_{bio} of -24.6 ± 0.2. These values are identical to the overall average.

In contrast to model derived values of discrimination, there is no discernable trend in δ_{bio} with latitude. Fung et al. (1997) used a biophysical model and found that discrimination changed from 10 to 20‰ between 30 and 50°N; values from the Suits et al. (personal communication, 2002) spanned 16–18.5‰, and those from Lloyd and Farquhar ranged between 15 and 16.5‰ over the same latitudes. The map of discrimination values used later in this study, which has been previously used to calculate the terrestrial carbon flux from NOAA/CMDL atmospheric observations (Ciais et al., 1995) ranges between 18 and 19‰ over the same latitudes. The average discrimination values we infer from observations are substantially less than the model values used in Ciais et al. (1995), with only two sites agreeing well. However, the most striking contrast is with the result of Fung et al. (1997). Our data do not support the large meridional gradient calculated in that study, as was already noted by Bakwin et al. (1998).

Our data agree best with the zonally averaged values from Lloyd and Farquhar and Suits et al.

3.2. Zonal variations

Although there are no obvious meridional trends in δ_{bio}, there are significant zonal variations. For this analysis, we divide the sites by continent: North America (ITN, LEF, NWR and UTA); Europe (ASK, BAL, BSC, HUN and WIS; note that "Europe" includes one site each from Africa and the Middle East); and Asia (KZM, KZD, TAP, UUM and WLG). Using weighted means, δ_{bio} for North America is 23.6 ± 0.3‰ (standard error of the mean), for Europe it is -25.0 ± 0.2‰ and for Asia it is -25.0 ± 0.3‰. The difference between the North American average and the European and Asian averages is significant ($P < 0.001$). In terms of discrimination (and assuming -8.0 per mil as the atmospheric starting point), the averaged δ_{bio} values correspond to 15.6 for North America, 17.0 for Europe and 17.0‰ for Asia. This pattern is consistent with differences between the continents in the model of Lloyd and Farquhar, where Eurasia tends to have higher discrimination values than North America. The summertime (May–September) $\delta^{13}C$ values of recently added biomass in the model of Suits et al. for temperate (30–50°N) North America, Europe and Asia are -23.9, -25.6 and -24.3. The agreement between the modeled and "observed" results for North America and Europe are very strong and are most likely due to greater C_4 photosynthetic activity in temperate North America, especially as a result of agriculture. The model results for Asia include areas of C_4 productivity, whereas the Asian sampling sites may be sampling air more from C_3 regions. We note that while the zonal differences in the model can be attributed to C_3 versus C_4 differences, the differences in our data could also be explained by climatic or species effects. Nonetheless, the overall agreement between our results and those of both Lloyd and Farquhar and Suits et al. is encouraging.

3.3. Temporal variations

Most analyses of discrimination have not accounted for interannual variations. However, there is good reason to expect that discrimination should vary from year to year in response to changes in environmental variables like rainfall and temperature (Farquhar et al., 1989). The estimated uncertainty for δ_{bio} for a single year is 2–3 times the size of that when all the data is taken together. Thus, discerning interannual variations is difficult for a single site. No individual sites exhibit statistically significant linear trends in δ_{bio} between the beginning and end of its record, but some sites exhibit interannual variability. Since the annual analysis at any given site is noisy, we bin the sites all together and by continent as in section 3.2, and then analyze the data annually. The results are shown in Fig. 4. When all sites are taken together there is surprisingly little interannual variability. Even when the data are divided by continent, only North America appears to have any meaningful variability; there is about a 3‰ increase in the North American δ_{bio} average between 1995 and 2000. This increase does not appear to be driven by any one site; the increase appears clearly only in the average. A temporal change of 3‰ is surprising given the relatively small degree of spatial variability in δ_{bio}.

In order to assess the effect of El Niño on δ_{bio}, we divided the data into El Niño and non-El Niño months, using $+1\,^{\circ}C$ of the Niño 3.4 combined index (Trenberth, 1997) as the division line. We then calculated δ_{bio} at each site, for all sites binned together, and for each binned continental region. These results are shown in Table 2. When the sites were binned all together or in regions, we found no significant difference between El Niño months and non-El Nino months. Among the sites, δ_{bio} of NWR changed from -23.0 ± 0.6 to -29.4 ± 2.9‰ and UUM changed from -23.3 ± 0.8 to -31.4 ± 2.7‰. No other sites exhibited significant changes ($P < 0.05$). It should first be noted that for sites that have no $\delta^{13}C$ data prior to 1994, the El Niño analysis is only an analysis of the El Niño period during the summer of 1997. This applies to most sites, but not NWR. The absence of a broad El Niño signal in our δ_{bio} values is perhaps not surprising because the sampling stations used in this study all lay outside of the tropics, where the most intense climatic effects of El Niño are seen. The reduction in the value of δ_{bio} at NWR and UUM could be indicative of reduced moisture stress on C_3 plants or a shift in the proportion of C_4:C_3 photosynthesis. Given the magnitude of the shifts, the second option may be more likely.

3.4. Comparing δ_{bio} with modeled photosynthetic discrimination

Comparing our δ_{bio} data to modeled values of discrimination involves several assumptions. First, we are comparing our δ_{bio} data that are representative of an ill-defined spatial area to model data that represent one particular grid cell. As discussed earlier, the design of our study attempts to minimize this problem,

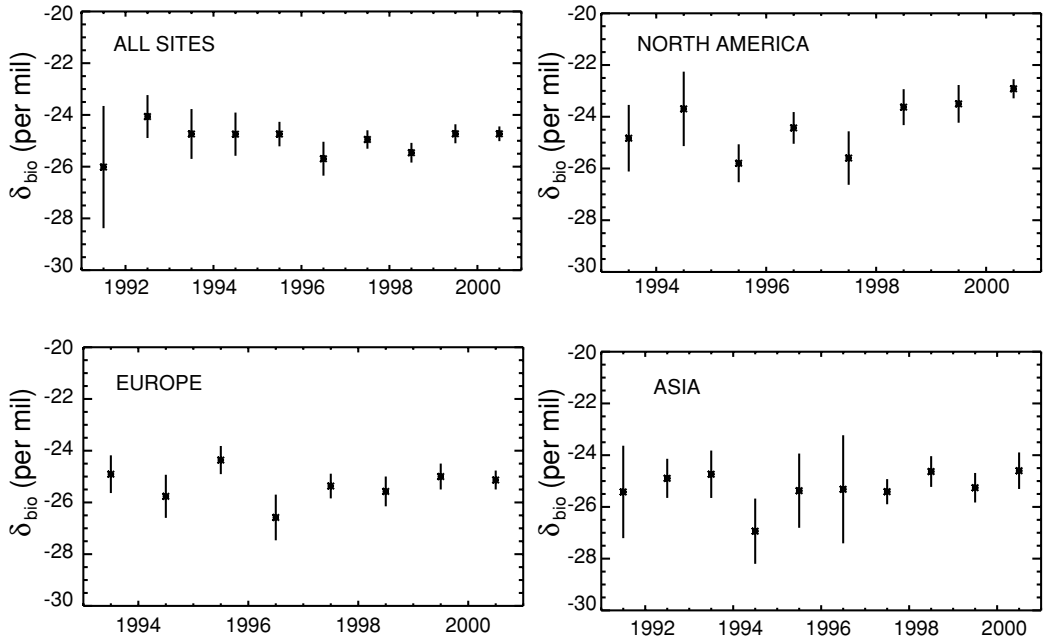

Fig. 4. Year-by-year values of the terrestrial isotopic signature for four sets of binned sites: all sites, Europe, Asia and North America.

Table 2. *Influence of El Niño on* δ_{bio}

Site	Niño 3 + 4 < 1.0C	Uncertainty	Niño 3 + 4 > 1.0C	Uncertainty	All data	Uncertainty	$P < 0.05$?
ASK	−26.78	1.54	−48.61	14.36	−27.67	1.62	No
BAL	−26.07	0.29	−25.57	1.34	−25.96	0.31	No
BSC	−22.93	0.79	−25.48	3.04	−23.02	0.76	No
HUN	−23.90	0.46	−24.05	0.82	−23.50	0.45	No
ITN	−24.47	0.61	−24.54	0.91	−24.49	0.55	No
LEF	−24.36	0.58	−25.24	1.55	−24.43	0.53	No
NWR	−23.01	0.64	−29.44	2.90	−23.23	0.62	Yes
TAP	−24.70	0.71	−25.05	0.68	−25.16	0.55	No
UTA	−20.19	0.91	−20.83	1.75	−20.23	0.82	No
UUM	−23.26	0.78	−31.41	2.72	−23.74	0.76	Yes
WIS	−24.29	1.21	−26.02	2.34	−24.46	1.09	No
WLG	−26.23	1.01	−24.60	1.14	−26.15	0.90	No

but we cannot be sure that our estimates of δ_{bio} represent areas close to the sampling stations. Nonetheless, it is unlikely that our atmospheric data could still be consistent with the large surface gradient of discrimination calculated by Fung et al. (1997). Second, we are assuming that the atmospheric starting point for photosynthetic discrimination is roughly −8‰, the approximate atmospheric average. Recycling of respired CO_2 in forest canopies could make the starting point significantly more negative than −8‰, which would make our inferred discrimination values smaller. For example, if the canopy atmosphere were −9‰ (instead of −8‰) and δ_{bio} were −24‰ this would result in a discrimination value of 15‰ (instead of 16‰). Seasonal changes in atmospheric $\delta^{13}C$ as well as Rayleigh distillation of $\delta^{13}C$ in the canopy would also have small effects of the conversion of δ_{bio} to photosynthetic discrimination.

Finally, we are converting δ_{bio} to photosynthetic discrimination even though δ_{bio} is a weighted average of the signatures of photosynthetic, respiratory and fossil fuel fluxes. During the summer, it is likely that the biological component is dominant, but fossil fuel fluxes will still play some role. If we first assume that photosynthetic and respiratory fluxes carry the same isotopic signature (i.e. no isotopic disequilibrium), we can examine the possible effect of δ_{ff} on δ_{bio} during the summer. δ_{ff} is always associated with a positive flux to the atmosphere and δ_{bio}, during the summer, is associated with a net negative flux. Assuming that δ_{ff} is lighter than δ_{bio}, this means, counter-intuitively, that δ_{bio} is too positive (Miller and Tans, 2002). However, given that there is no significant difference between summertime δ_{bio} with and without the fossil fuel correction, this effect is probably small. Because of the isotopic disequilibrium between soil carbon and the atmosphere induced by fossil fuel emissions, the annual average isotopic signature associated with respiration is probably systematically heavier than the photosynthetic signature in most areas. If we assume a 0.4‰ disequilibrium, and a ratio of photosynthetic to respiratory fluxes of 1.5:1, then our current estimates of δ_{bio} would be too negative by about 0.2‰. This potential correction is in the opposite direction of that for fossil fuel. Nonetheless, it is important to remember that δ_{bio} is an average of the isotopic signatures associated with photosynthetic and respiratory fluxes.

4. Implication of δ_{bio} on land/Ocean flux partitioning

Following the method of Ciais et al. (1995), we use a simple two-dimensional inverse model to calculate zonally averaged terrestrial and oceanic net surface fluxes of CO_2. The oceanic disequilibrium used is based on surface ocean $\delta^{13}C$ measurements (Kroopnik et al., 1977), and the terrestrial disequilibrium term was derived using the CENTURY soil model (Ciais et al., 1995). The sum of the disequilibrium terms is close to the value of 89 GtC ‰ yr^{-1} calculated by Battle et al. (2002) using O_2/N_2, CO_2 and $\delta^{13}C$. To test the sensitivity of the flux partitioning to discrimination, we ran the model with a discrimination map that more closely matched our observations. In the region of our observations, we adjusted the discrimination to 16.5‰, and in all other regions we reduced discrimination by 1‰, on the basis that the discrimination model might be systematically biased toward larger values of discrimination. As seen in Table 3, reducing discrimination in the northern temperate zone by about 1.5‰ increases the terrestrial sink by about 0.4 GtC yr^{-1}. The effects are minimal in other zones.

The effect of inter-annual changes in discrimination was not investigated, but would certainly be important. The effect of interannual changes in discrimination is two-fold. First is the straightforward effect as documented above. Second, is the indirect effect that changing discrimination would have on terrestrial disequilibrium (James Randerson, personal communication). For the fraction of soil carbon that has a residence time close to 1 yr, its disequilibrium with the atmosphere when respired would by equal to the difference in photosynthetic discrimination in the following year. This could have a substantial impact on the inter-annual calculation of fluxes.

5. Conclusion

Using correlations between anomalies in $\delta^{13}C$ and CO_2, we have calculated isotopic signatures for the terrestrial biosphere in the temperate Northern Hemisphere. Our principal interest in the value of the signatures is in their use as parameters in the partitioning of oceanic and terrestrial fluxes of CO_2. Since the continental sites in the NOAA/CMDL Cooperative Air Sampling Network are restricted to a relatively small band of latitudes in the Northern Hemisphere, our approach cannot be used to provide a global set

Table 3. *Inversely derived oceanic and terrestrial CO_2 fluxes*

1991–2001	90–54°S	53–18°S	17°S–17°N	18–53°N	54–90° N
Total	0.05	−1.40	1.66	−2.70	−0.26
Ocean	0.07	−1.60	0.64	−1.04	−0.39
Land	−0.02	0.20	1.01	−1.65	0.13
Land with "observed" discrimination	−0.03	0.21	1.08	−2.02	−0.05

of isotopic signatures. Thus, we have compared our calculated signatures with various model-derived values for discrimination. In doing so, we have gained some sense of the relative strengths and weakness of the models. It bears repeating that it is difficult to compare directly our signatures with model photosynthetic discrimination because: (1) the isotopic signature associated with respiration is always included in our samples, and (2) our signatures do not correspond with well defined areas on the earth's surface. Even with these caveats, we think that our approach is an important way to use atmospheric observations to assess modeled values of discrimination on large spatial scales. Finally, as CO_2 and $\delta^{13}C$ data are collected more frequently and in more places, we should be able to apply our methods to understand better temporal and spatial variability of $\delta^{13}C$ fractionation.

6. Acknowledgements

We wish to thank the analysts at NOAA/CMDL and University of Colorado/INSTAAR for analyzing the air samples, and the sample takers for collecting the air samples used in this study. John Miller was supported by a National Research Council Postdoctoral Fellowship during this work.

REFERENCES

Andres, R. J., Marland, G. and Bischof, S. 1996. Global and Latitudinal Estimates of ^{13}C from Fossil-Fuel Consumption and Cement Manufacture. Carbon Dioxide Information and Analysis Center, http://cdiac.esd.ornl.gov/

Bakwin, P. S., Tans, P. P., White, J. W. C. and Andres, R. J. 1998. Determination of the isotopic (C-13/C-12) discrimination by terrestrial biology from a global network of observations. *Global Biogeochem. Cycles* **12**, 555–562.

Battle, M., Bender, M. L., Tans, P. P., White, J. W. C., Ellis, J. T., Conway, T. and Francey, R. J. 2000. Global carbon sinks and their variability inferred from atmospheric O_2 and ^{13}C. *Science* **287**, 2467–2470.

Ciais, P., Tans, P. P., White, J. W. C., Trolier, M., Francey, R. J., Berry, J. A., Randall, D. R., Sellers, P. J., Collatz, J. G. and Schimel, D. S. 1995. Partitioning of ocean and land uptake of CO_2 as Inferred by delta-C-13 measurements from the NOAA Climate Monitoring and Diagnostics Laboratory Global Air Sampling Network. *J. Geophys. Res.* **100**, 5051–5070.

Conway, T. J., Tans, P. P., Waterman, L. S., Thoning, K. W., Kitzis, D. R., Massarie, K. A. and Zhang, N. 1994. Evidence for interannual variability of the carbon cycle for the National Oceanic and Atmospheric Administration/Climate Monitoring Diagnostics Laboratory Global Air Sampling Network. *J. Geophys. Res.* **99**, 22,831–22,855.

Farquhar, G. D., Ehleringer, J. R. and Hubick, K. T. 1989. Carbon Isotope Discrimination During Photosynthesis. *Ann. Rev. Plant Physiol. Plant Mol. Biol.* **9**, 121–137.

Fung, I., Field, C. B., Berry, J. A., Thompson, M. V., Randerson, J. T., Malmstrom, C. M., Vitousek, P. M., Collatz, G. J., Sellers, P. J., Randall, D. A., Denning, A. S., Badeck, F. and John, J. 1997. Carbon 13 exchanges between the atmosphere and biosphere. *Global Biogeochem. Cycles* **11**, 507–533.

Gloor, M., Bakwin, P., Hurst, D., Lock, L., Draxler, R. and Tans, P. 2001. What is the concentration footprint of a tall tower? *J. Geophys. Res.* **106**, 17,831–17,840.

Keeling, C. D. 1961. The concentrations and isotopic abundances of atmospheric carbon dioxide in rural and marine air. *Geochim. Cosmochim. Acta*, **24**, 277–298.

Kroopnik, P. M., Margolis, S. V. and Wong, C. S. 1977. In: *The fate of fossil fuel in the oceans* (eds. N, Anderson and A. Malahoff) Plenum, New York, 295–321.

Lloyd, J. and Farquhar, G. D. 1994. C-13 discrimination during CO_2 assimilation by the terrestrial biosphere. *Oecologia* **99**, 201–215.

Marland, G., Andres, R. J. and Boden, T. A. 1993. In: *Trends '93: A compendium of data on global change*, Vol. ORNL/CDIAC-65 (eds. T. A. Boden, D. P. Kaiser, R. J. Sepanski and F. W. Stoss) Carbon Dioxide Info. Analysis Center, Oak Ridge Natl. Lab., Oak Ridge, Tenn., 505–584.

Miller, J. B. and Tans, P. P. 2002. Calculating isotopic discrimination from atmospheric measurements at various scales. *Tellus* **55B**, this issue.

Novelli, P. C., Masarie, K. A. and Lang, P. M. 1998. Distributions and recent changes of carbon monoxide in the lower troposphere. *J. Geophys. Res.* **103**, 19 015–19 033.

Potosnak, M. J., Wofsy, S. C., Denning, A. S., Conway, T. J., Munger, J. W. and Barnes, D. H. 1999. Influence of biotic exchange and combustion sources on atmospheric CO_2 concentrations in New England from observations at a forest flux tower. *J. Geophys. Res.* **104**, 9561–9569.

Tans, P. P. 1980. On calculating the transfer of carbon-13 in resevoir models of the carbon cycle. *Tellus* **32**, 464–469.

Tans, P. P., Berry, J. A. and Keeling, R. F. 1993. Oceanic $^{13}C/^{12}C$ observations: A new window on ocean CO_2 uptake. *Global Biogeochem. Cycles* **7**, 353–368.

Thoning, K. W., Tans, P. P. and Komhyr, W. D. 1989. Atmospheric carbon dioxide at Mauna Loa Observatory 2. Analysis of the NOAA GMCC data, 1974–1985. *J. Geophys. Res.* **94**, 8549–8565.

Trenberth, K. E. 1997. The definition of El Nino. *Bull. Am. Meteorol. Soc.* **78**, 2771–2777.

Trolier, M., White, J. W. C., Tans, P. P., Massarie, K. A. and Gemery, P. A. 1996. Monitoring the isotopic composition of atmospheric CO_2: Measurements from the NOAA global air sampling network. *J. Geophys. Res.* **101**, 25 897–25 916.